Load Signature Study—Part II: Disaggregation Framework, Simulation, and Applications

Jian Liang, Simon K. K. Ng, *Member, IEEE*, Gail Kendall, and John W. M. Cheng, *Member, IEEE*

***Abstract*—Load signatures embedded in common electricity consumption patterns, in fact, could render much information pertaining to the nature of the appliances and their usage patterns. Based on the proposed disaggregation framework, we use three advanced disaggregation algorithms, called committee decision mechanisms (CDMs), to perform load disaggregation at the metering level. Three random switching simulators are also developed to investigate the performance of different CDMs under a variety of scenarios. Through Monte Carlo simulations, we demonstrate that all CDMs outperform any single-feature, single-algorithm-based disaggregation methods. With sensitivity analysis, we also show that the CDMs are less sensitive to any load dynamics and noise. We finally demonstrate some applications of this technology in terms of appliance usage tacking and estimated energy consumption of each appliance.**

***Index Terms*—Committee decision mechanism, electric-load intelligence, load disaggregation, load signature, Monte Carlo methods, smart metering.**

I. Introduction

THE challenges of load disaggregation based on load signatures [1]–[5] are three fold. First, the underlying load signatures making up the composite load are similar to each other in terms of all or part of their features. Second, the load has dynamic characteristics within it such that minor fluctuations exist continuously. Third, the composite load is also subjected to noise due to the dynamic nature of supplying power system and the interference of the surrounding environment.

In general, although two appliances may have similar features, other features could have detectable traits so that they can be used for identification. For instance, a water boiler and air conditioner may look the same in their steady-state signatures but their transient features are noticeably different. Furthermore, different disaggregation algorithms have different recognition capabilities which depend on the features being analyzed. As such, this paper first presents a framework for load disaggregation using three committee decision mechanisms (CDMs). We also propose different random appliance switching simulators and illustrate how these simulators can help us evaluate the performance of different load disaggregation methods, particularly the CDMs. A load dynamic model is also incorporated in the study to make the simulations more realistic. We then discuss the key findings from the simulations and associated sensitivity analyses. Finally, we present some potential application ideas for smart metering and offer an outlook of future research.

Manuscript received August 28, 2008; revised May 25, 2009. First published November 17, 2009; current version published March 24, 2010. This work was supported by the CLP Research Institute Ltd. Paper no. TPWRD-00654-2008.

The authors are with the CLP Research Institute Ltd., Hong Kong (e-mail: jian.liang@clp.com.hk; simonkkng@clp.com.hk; kendall@clp.com.hk; john.cheng@clp.com.hk).

Color versions of one or more of the figures in this paper are available online at http://ieeexplore.ieee.org.

Digital Object Identifier 10.1109/TPWRD.2009.2033800

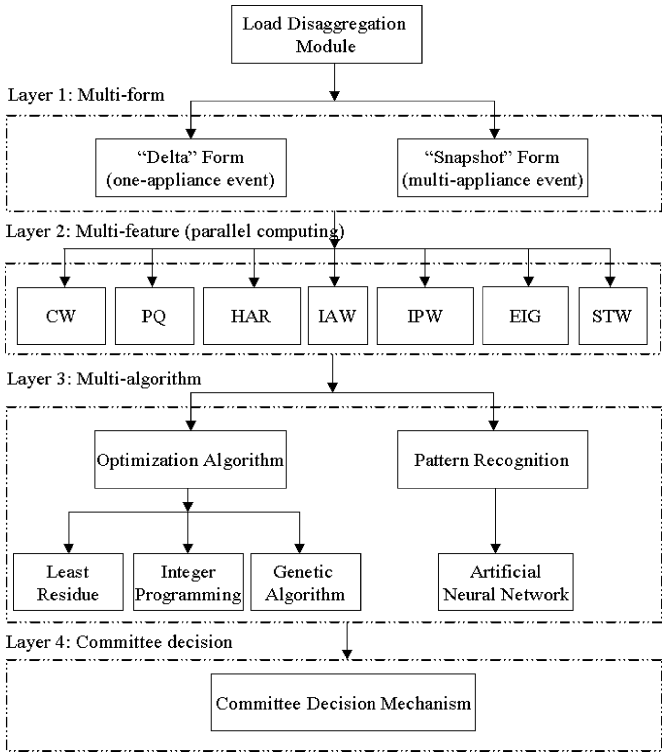

Fig. 1. Load disaggregation framework.

II. Load Disaggregation Framework

Fig. 1 shows a four-layer load disaggregation framework which is suitable for load disaggregation at the metering level. In the first layer, load signatures in either "Delta" form or "Snapshot" form could be used. In this paper, we have used the delta form because it is more distinct and easier for feature extraction. In the second layer, different features in transient and steady-state behaviors are extracted in multiple domains, including current waveform (CW), active/reactive power (PQ), harmonics (HAR), instantaneous admittance waveform (IAW), instantaneous power waveform (IPW), eigenvalues (EIG) and switching-transient waveform (STW). In the third layer, both optimization algorithms (e.g., least residue (LS), and pattern recognition methods, for example, artificial neural network (ANN)) are used for load disaggregation. Finally, by incorporating the solutions from the single-feature single-algorithm approaches, three CDM methods (proposed in the first part of

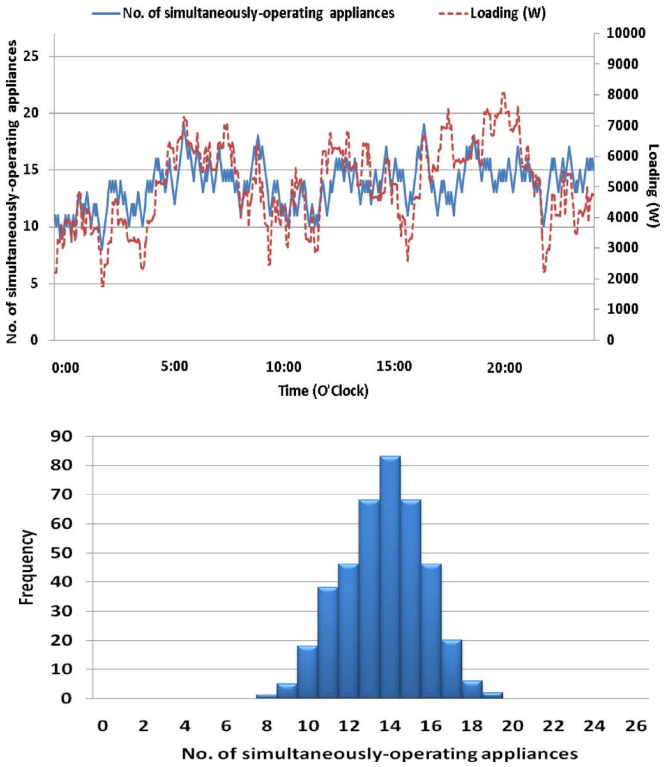

Fig. 2. (a) Simulation result of the normally distributed simulator. (b) Histogram of the number of simultaneously operating appliances of the normally distributed simulator.

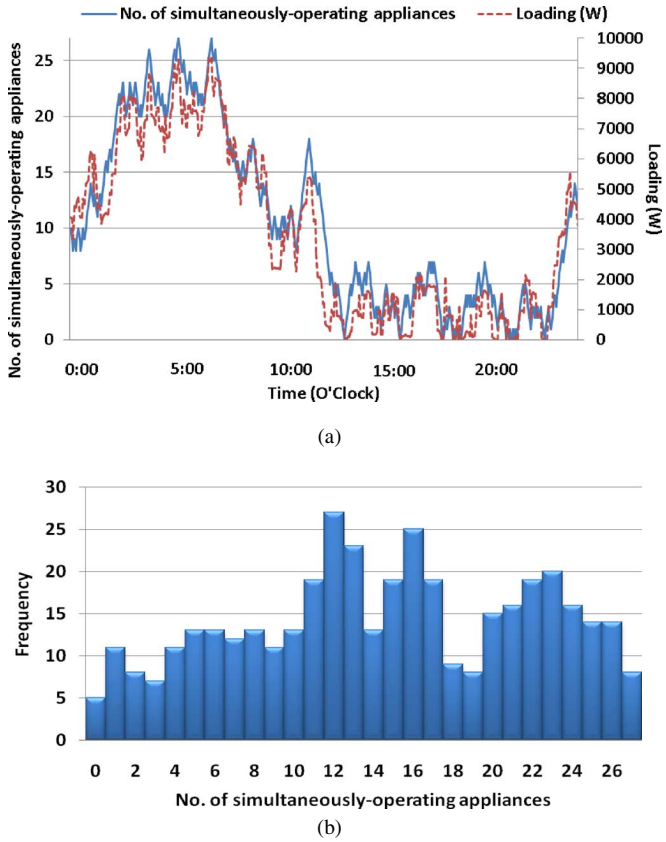

Fig. 3. (a) Simulation result of an evenly distributed simulator. (b) Histogram of the number of simultaneously operating appliances of an evenly distributed simulator.

this two-part paper), named most common occurrence (MCO), least unified residue (LUR), and maximum-likelihood estimation (MLE), are utilized to render the best answer possible. Therefore, this framework establishes a multifeature and multialgorithm platform to identify individual appliances and their usage patterns.

III. Advanced Simulator Design

Since it is impractical to conduct actual trials for thousands of different scenarios, we have devised a number of simulators by using typical random number generation functions in Matlab and Monte Carlo methods [6]. Simulations are constructed by summing up individual appliance signatures from a database of 27 typical appliances and a total of 32 operating modes as shown in the Appendix in the first part of this two-part paper. The simulation results are then used to examine the CDM disaggregation performance in millions of simulations. This section explains the architecture of different simulators.

A. Random Switching Generation

We used three different types of probabilistic distribution functions for the switching events, namely, normally distributed, evenly distributed and behavioral based. Though not necessarily lifelike, the simulations are designed to generate millions of distinctly different scenarios. We used these simulations to test different algorithms for accuracy and reliability in disaggregating composite loads and/or identifying appliances as they are switched on or off.

1) Simulator I: Normally Distributed: This simulator generates a series of random switching with any prescribed time interval. At the end of each time interval, this simulator randomly chooses an appliance and then toggles its current operating state to the opposite state. The resulting behavior will give normally distributed behavior in terms of the number of simultaneously operating appliances as shown in Fig. 2(a) and (b).

2) Simulator II: Evenly Distributed: This simulator also generates a series of random switching with a prescribed time interval. However, at each time interval, this simulator first randomly chooses whether we want to turn "on" or "off" an appliance. If it is an "on" state selected, we will randomly select an appliance which is presently off and then turn it on. If none of the appliances are off, we will just randomly choose one to switch it off and so on. Fig. 3(a) and (b) shows the simulation result and the histogram of the number of simultaneously operating appliances, respectively. In contrast to the normally distributed Simulator I, the number of simultaneously-operating appliances of this simulator is more evenly distributed as shown in Fig. 3(b). As shown in Fig. 2(a) and (b), the mean number of simultaneously-operating appliances for both simulators I and II are 13 (out of a database of 27 appliances), but Simulator II has a larger standard deviation in terms of simultaneously operating appliances. In comparison with Simulator I, Simulator II gives more variety in terms of total numbers of appliances operating simultaneously.

3) Simulator III: Behavioral Based: This simulator is designed to produce more realistic consumption patterns of different household appliances during the day. First, we classify the database appliances into four types. (The classification and detailed procedures of this simulator are given in the Appendix). Second, we define the expected operating periods and the probabilities of each type being on during each time segment of a day. Some of them may be switched regularly and frequently (e.g., refrigerator) and some may be switched occasionally (e.g., hair dryer or water boiler). The frequency of usage of each appliance during the simulation is determined by their preset probabilities which are elaborated in the Appendix. Fig. 4(a) and (b) shows a typical simulation result and the histogram of the number of simultaneously-operating appliances, respectively. Simulations from behavior-based simulator III are more representative of typical household power consumption, such as the one shown in Fig. 4(c).

B. Initial Conditions

A random initial condition is set for normally distributed and evenly distributed simulators (Simulator I and II), and every appliance has an equal chance of being chosen to be on. However, the initial condition for the behavioral-based simulator (Simulator III) depends on the probability assigned for each appliance at the starting time. The initial and final conditions are not significant in the simulation because they only constitute a small portion of the overall simulation.

C. Load Dynamics Simulation

In this paper, load dynamics is defined as "the small fluctuation of individual load signature which is intrinsic to the natural operation of an appliance." For instance, Fig. 5(a) shows a set of overlaying load signatures collected from an air conditioner. It is apparent that there is an envelope within which the load signatures will vary dynamically even within each cycle. Fig. 5(b) shows the load signatures of an air conditioner taken over 5 s. The load dynamic envelope can be easily seen as well. In the frequency domain, certain harmonic contents at 100 Hz from air conditioners (ID 1 and 2 in Fig. 5(c)) are noticeably different from other appliances [ID 3 to 20 in Fig. 5(c)]. For other motor-driven appliances, such as the dehumidifier (ID 6), refrigerator (ID 17), and microwave oven (ID 16), they also exhibit similar harmonic contents but the magnitudes are much smaller. Given these characteristics, this paper proposes a method to model load dynamics by using the harmonic contents and Monte Carlo methods as described in the following sections.

First of all, the CW signature of an appliance is analyzed by using fast Fourier transformation (FFT). The frequency components in rectangular coordinates ($X(f_k) = a_k + jb_k$) are shown in Fig. 6. By emulating the fluctuation magnitude of a_k and b_k within a range we defined here as the load-dynamics-magnitude (LDM), the load dynamics could be simulated in the time domain using inverse FFT as in (1), shown at the bottom of the page, where $x(t_{\rm n})$ is the simulated current waveform in the time domain with built-in load dynamic features, and $rand(\,)$ is a random number generator with a set boundary conditions. For different appliances, this LDM differs in magnitude as well as its associated frequencies. Thus, the upper and lower bounds of the coefficient a_k and b_k for individual appliance are derived from the database values. By varying the magnitude of LDM, we can also change the level of fluctuation as well. It should be noted that some special appliances, such as the air conditioner, exhibit periodic load dynamics as shown in Fig. 5(b). Based on the frequency analysis, it is found that the phase relationship between a_k and b_k always follows a specific pattern at certain frequencies, and these behaviors are also emulated herein.

D. Noise Simulation

In this paper, noise is modeled by a signal-to-noise ratio (SNR). Herein, the noise can be implemented by adding some zero-mean random noise with the magnitude being proportional to the aggregated power.

E. Simulation Settings

Based on the developed simulators, load dynamics and noise models, a series of simulations was conducted in this paper. During the simulation process, settings are made as follows.

1) The simulated composite load is made up entirely of known appliances from a given database (as shown in the Appendix in the first part of this two-part paper).
2) Only one appliance will be switched at a time (i.e., at most, one appliance is switched between two sequential snapshots).
3) The delta form load signature between two sequential snapshots is used for load disaggregation.
4) Event detection would use $\mathrm{P} > 100$ W as a threshold to identify any significant switching as an event. Correspondingly, only the appliances (>100 W) will be recognized.
5) For simplicity, the multimode appliances, such as hair dryer and induction cooker, are not allowed any mode-to-mode changes during the operation unless they first go through an off stage.

F. Simulation Procedures

In this paper, the simulation program is based on generating 400 switchings of power-hungry appliances (>100 W per ap-

$$x(t_{\rm n}) = \frac{1}{2}\sum_{k=0}^{N-1}\{[(a_{k,H}-a_{k,L}) + rand(-LDM, LDM)\times(a_{k,H}-a_{k,L})] + j[(b_{k,H}-b_{k,L}) + rand(-LDM, LDM)\times(b_{k,H}-b_{k,L})]\}e^{j2\pi kn/N} \quad (1)$$

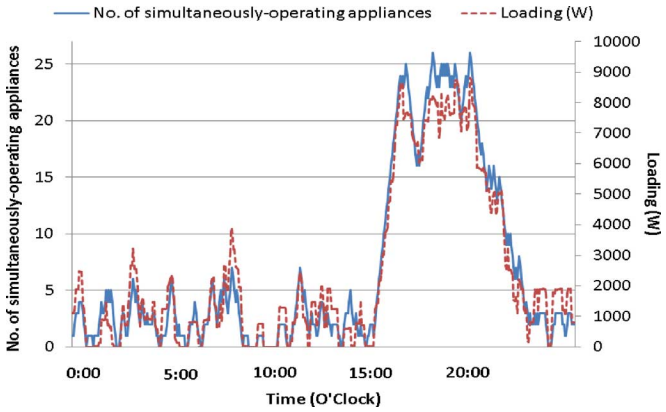

(a)

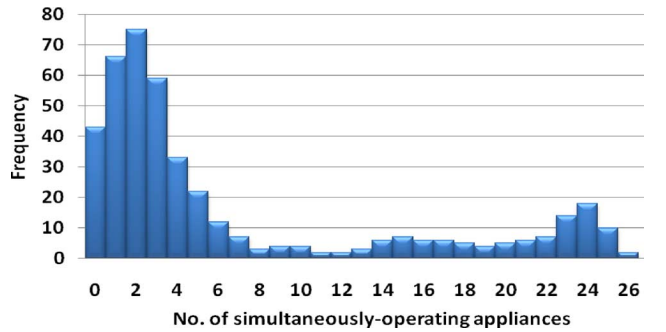

(b)

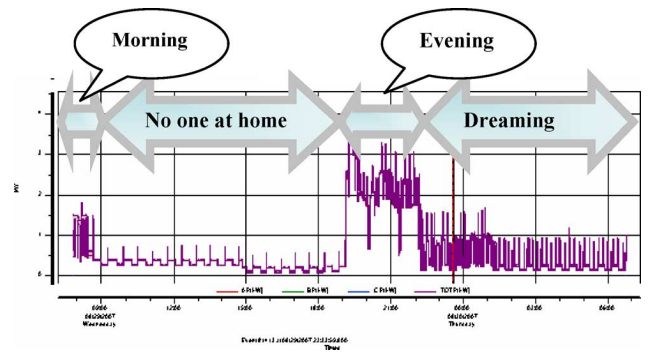

(c)

Fig. 4. (a) Simulation result of the behavioral-based simulator. (b) Histogram of the number of simultaneously-operating appliances of the behavioral-distributed simulator. (c) Typical power consumption of a household.

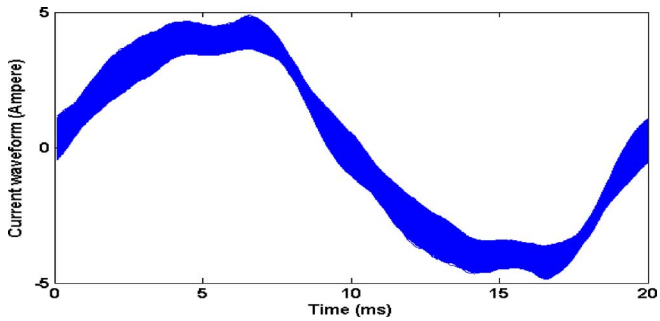

(a)

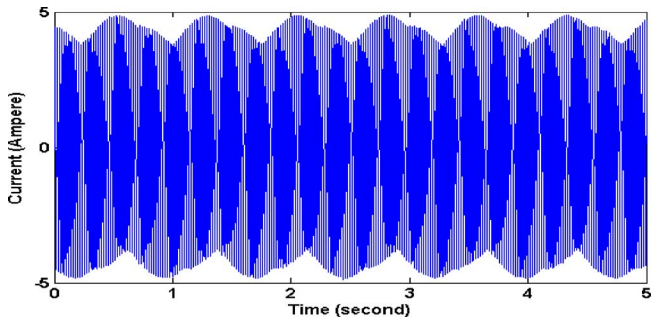

(b)

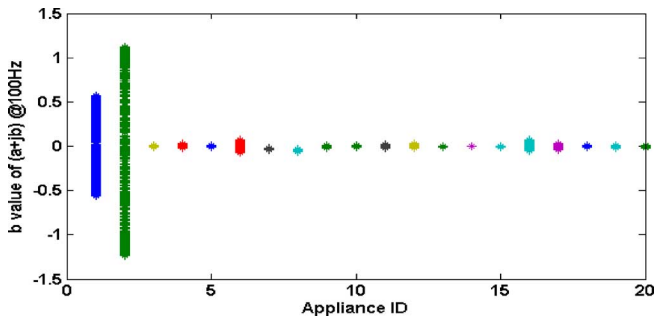

(c)

Fig. 5. (a). Air conditioner CW under different cycles. (b). Air conditioner CW in 5 s. (c). Harmonics feature under different cycles.

pliance) per case (equivalent to a day) and repeated for 30 cases (equivalent to a month). In other words, each simulation has a total of 12 000 events. In each case, procedures are noted as follows.

1) A sufficiently large amount of random switchings (i.e., at least 400 large appliance switchings and a number of small appliance switchings included) are first generated from the selected simulator (e.g., I, II, or III).
2) Based on the generated switchings, we reconstruct the equivalent snapshots of the composite load incorporating the on/off switchings, load dynamics, and noises. It should be noted that the snapshot interval is like the sampling period in real life (e.g., every second) so it may be much smaller than an event interval (e.g., minutes or hours apart).
3) The Event Detection Module extracts load signatures in the delta form (between sequential snapshots) and judges whether there is an event.
4) Based on the detected events, the feature extraction and load disaggregation programs are executed.
5) By comparing the known simulated events and the disaggregation results, the performance is evaluated by using the disaggregation accuracy indices defined in Part I of this two-part paper.

The choice of 400 events per case and 30 cases is arbitrary for our simulation. It will be illustrated in the following section that these settings would ensure convergence of the results.

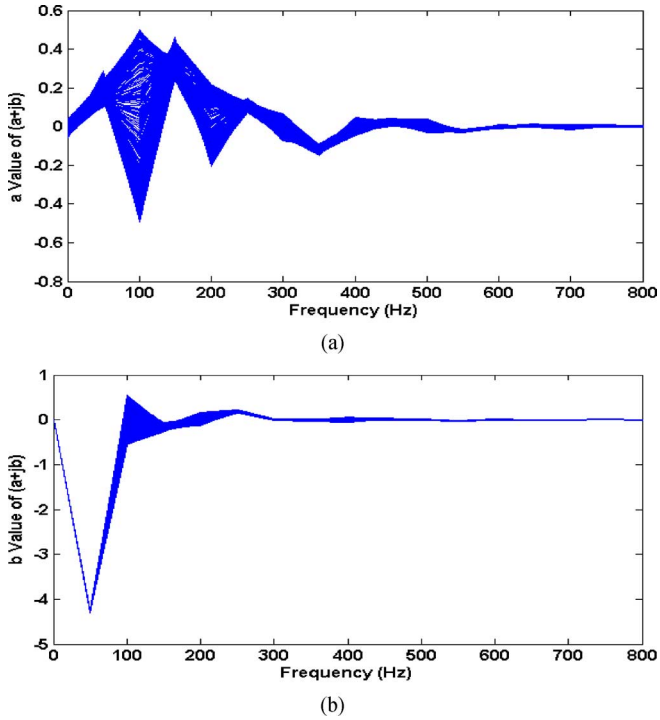

Fig. 6. Air-conditioner frequency features ($a + jb$) under different cycles. (a) Real part a. (b) Imaginary part b.

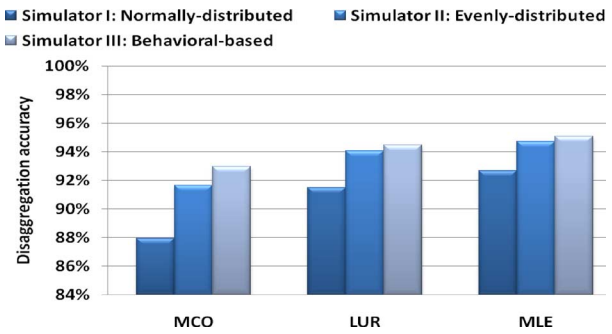

Fig. 7. Disaggregation performance of different simulators.

IV. Simulation Results

A. Performance of Different Simulators

Fig. 7 shows that the accuracies of different CDMs vary with respect to the type of simulators. In other words, accuracy is dependent on the set of simulations used for testing. Fig. 7 shows that of the three simulators, Simulator I was the most challenging for all CDM algorithms. It also shows that of the three CDMs, MCO was the least accurate, LUR was better, and MLE was the best in all three sets of simulations.

B. Detailed Performance Analysis

Our study also included testing the algorithms on simulations that included the noise and dynamic features characteristic of grid-connected power. Fig. 8 shows the results of Simulator I from single-feature, single-algorithm, and CDM. It was found that the disaggregation accuracies of the three proposed CDMs were higher than all other single algorithms under the simulation conditions in our study. By far, The MLE gave the best performance among the three CDMs and it could achieve a disaggregation accuracy of up to 92.7%. The second runner up was an LUR with an accuracy of 91.5%. It was then followed by MCO with an accuracy of 87.9% which was still better than all other individual algorithms, as shown in Fig. 8. In the simulation, the SNR and LDM are set at 100 dB and 1, respectively. This is used as our base case for further comparison purposes.

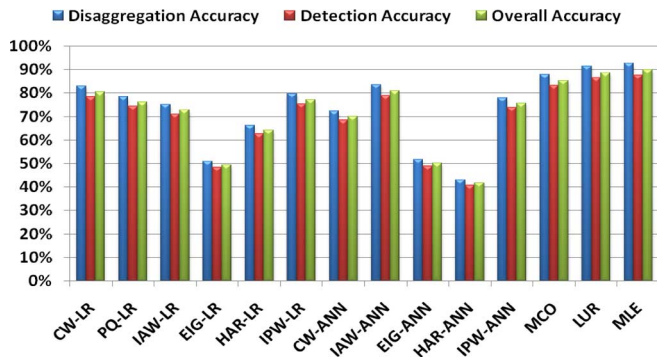

Fig. 8. Disaggregation performance of different algorithms.

V. Sensitivity Analysis

A. Impact of Load Dynamics and Noise

In practical situations, the noise and load dynamics levels will vary depending on the working environment and specific appliance characteristics. We have conducted a sensitivity analysis to investigate the disaggregation accuracy under different noise and load dynamics levels. Fig. 9(a) shows the disaggregation accuracies from Simulator I for LUR (one of the CDMs) when the SNR varied from 100 dB to 10 dB and LDM varied from 0 to 2.0. Fig. 9(b) shows the disaggregation accuracy of an algorithm using only the PQ feature and LR algorithm. Comparing Fig. 9(a) with (b), the LUR was clearly more robust than PQ-LR under different combinations of LDM and SNR. From the least perturbed (LDM = 0, SNR = 100 dB) to the noisiest (LDM = 2, SNR = 10 dB), it can be seen that the accuracy of PQ-LR dropped from 100% to around 50%. On the other hand, the accuracy of LUR was only reduced by about 20%. This again illustrated the robustness and reliability of the CDM method.

B. Impact of the Number of Events Per Day

Fig. 10 shows the disaggregation accuracy from Simulator I when the number of events increased from 1 to 600 per case (equivalent to a day). It was found that the accuracies from different algorithms varied significantly when the number of events was small. However, as the number of events increased, the accuracy stabilized. In our observation, the accuracy should best be measured over a large number of events (e.g., >200). It should be noted that the disaggregation accuracy would also vary slightly at different cases. In order to obtain a consistent level of accuracy, simulation should be run with a large number of events, for example, at least 200 events per case and 30 cases are repeated (a total of 6 000 events).

C. Impact of the Number of Simultaneously-Operating Appliances

Intuitively, the disaggregation accuracy should correlate with the number of simultaneously-operating appliances. Fig. 11

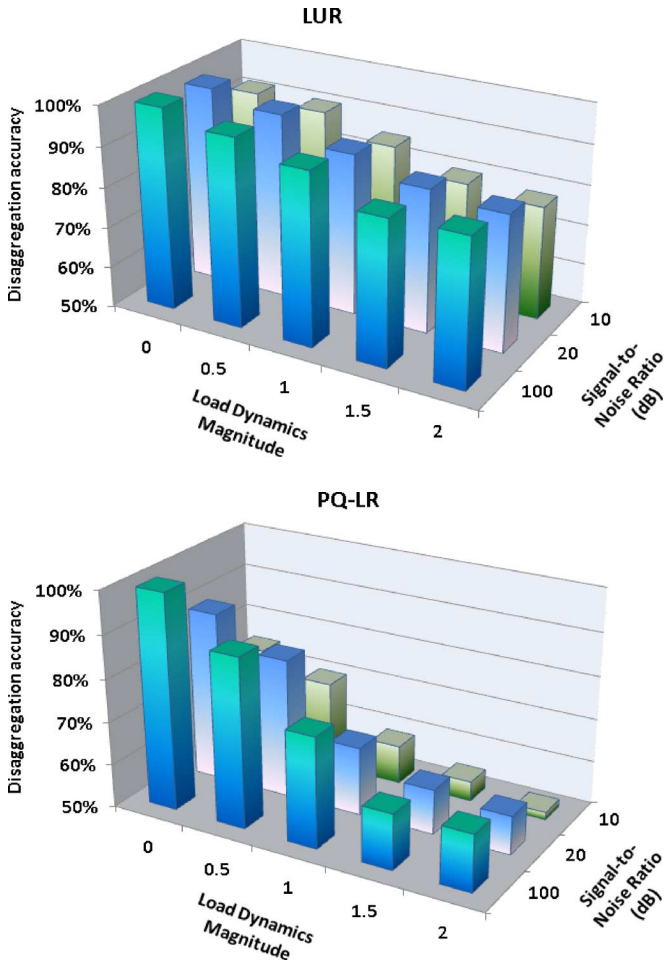

Fig. 9. (a) Disaggregation performance of the CDM (LUR) for different combinations of LDM and SNR. (b) Disaggregation performance of single feature-algorithm (PQ) for different combinations of LDM and SNR.

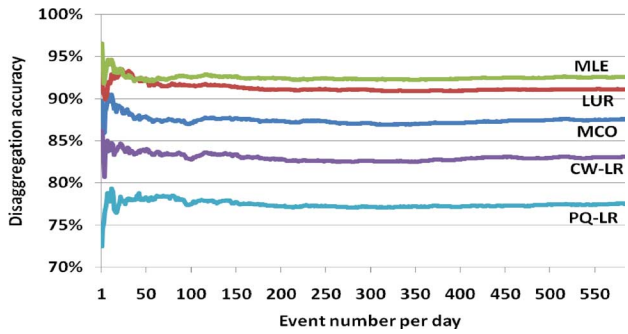

Fig. 10. Accuracies of a different number of events per day.

shows the disaggregation accuracy from Simulator I when the number of simultaneously-operating power-hungry appliances varied from 0 to 15. We can see that the accuracies for all algorithms were decreasing if the appliance number was increasing. This is attributed to the fact that the signals are more distorted if the number of simultaneously-operating appliances is high. MLE and LUR gave a very good result when there were only a few power-hungry appliances as shown in the first range $[0, 4)$ in Fig. 11.

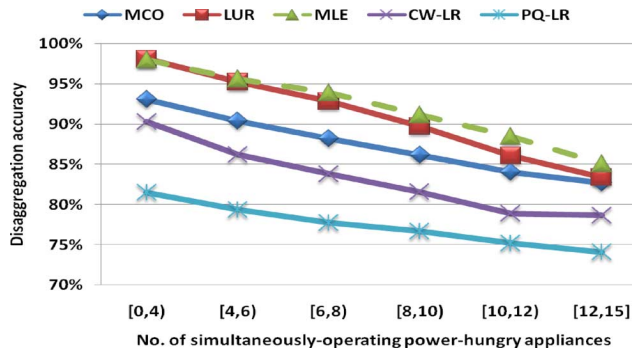

Fig. 11. Disaggregation performance of a different number of simultaneously-operating power-hungry appliances.

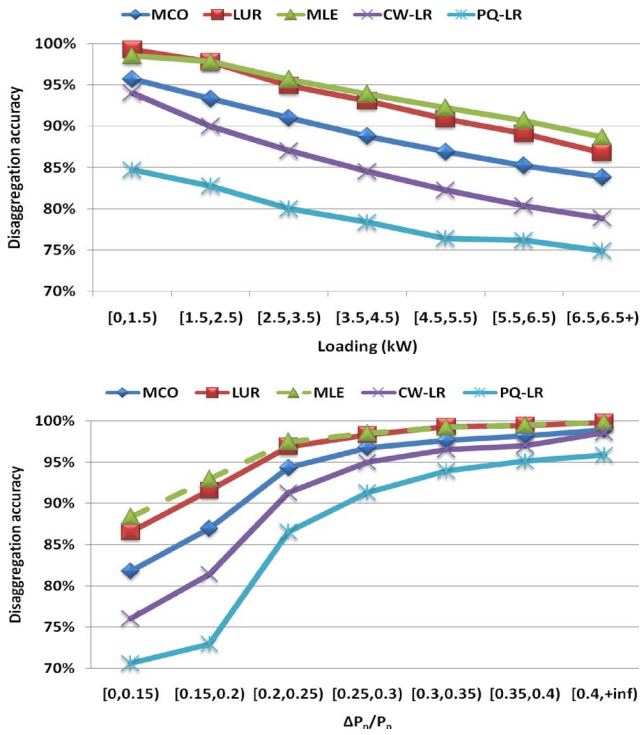

Fig. 12. (a). Disaggregation performance of different loading. (b). Disaggregation performance of a different load increment.

D. Impact of Loading and Load Increment

Loading is defined as the total consumption of all simultaneously-operating appliances at any given time. The load increment is defined as the incremental consumption added to loading when an appliance is switched on and vice-versa. As such, we can define a ratio $\Delta P_{\rm n}/P_{\rm n}$, where $\Delta {\rm P_n} = |{\rm P_{n+1}} - {\rm P_n}|$ is an incremental change between two consecutive snapshots and $P_{\rm n}$ is the total power of the previous snapshot. This ratio can be used to measure the impact of loading on disaggregation accuracy. Fig. 12(a) shows the disaggregation accuracy from Simulator I when all of the events were divided into seven ranges as shown in its horizontal axis. It is observed that the results from three CDM algorithms in Fig. 12(a) were quite similar to Fig. 11.

Fig. 12(b) shows the disaggregation accuracy from the same set of data with respect to the $\Delta P_{\rm n}/P_{\rm n}$ ratios. It is observed that the accuracy was the lowest if the ratio was small ranging from

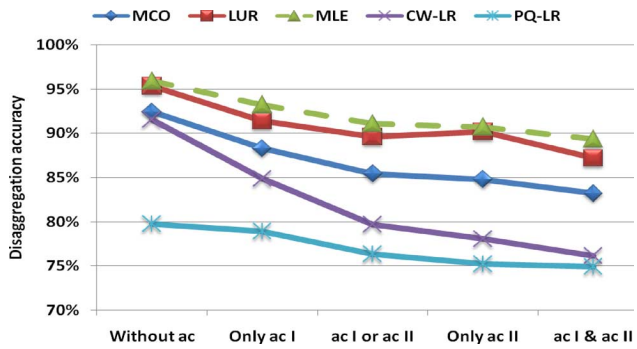

Fig. 13. Disaggregation performance with or without air conditioners.

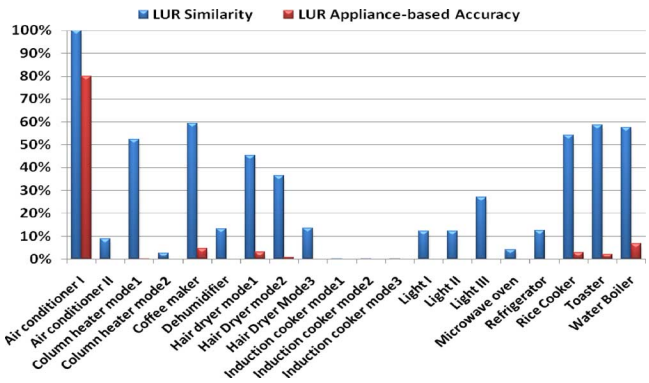

Fig. 14. Similarity versus appliance-based accuracy.

0 to 0.15 for all algorithms. This means the disaggregation accuracy is highly sensitive to existing loading. If the incremental load was large, say $\Delta P_{\rm n}/P_{\rm n}$ was more than 0.35, it can be seen that LUR and MLE could reach accuracies of nearly 100%. It should also be noted that the slope in Fig. 12(b) depends on the individual characteristics of appliances in the database.

E. Impact of Air Conditioners

In general, air conditioners consume 30%–50% of the household energy consumption [7]. Since it has periodical load dynamics and a special harmonics feature, air-conditioner tracking would be of particular interest to customers as well as suppliers. However, the inherent load dynamics from air conditioners will also affect the recognition of other appliances. Fig. 13 shows the disaggregation accuracy for events with or without air conditioners. The ac I and ac II in Fig. 13 correspond to the air conditioners I and II in the database as mentioned in the first part of this two-part paper. All algorithms, regardless of CDM or the individual feature algorithm, performed much better without air conditioners. For two air conditioners operating simultaneously, it can be seen that the accuracies of all algorithms were lower than when only one was operating. In Fig. 13, it is also clear that CW-LR was more likely to be affected by the presence of air conditioners (load dynamics) with a noticeable drop in accuracy. On the other hand, the CDMs were less sensitive.

F. Impact of Similarity

For the appliances with higher similarity with other appliances, their disaggregation accuracy will be poor, and vice-versa. In this paper, the similarity definition is further extended to include multifeatures using the LUR algorithm as

$$s_{(ia,ib)} = \prod_{j=1}^{M} s^{j}_{(ia,ib)} = \prod_{j=1}^{M} \left\{ \frac{\sum_{k=1}^{N} y^2_{k|(ia,j)}}{\left[\sum_{k=1}^{N} y^2_{k|(ia,j)} + \sum_{k=1}^{N} \left(y_{k|(ia,j)} - y_{k|(ib,j)} \right)^2 \right]} \right\} \quad (2)$$

where $s^{j}_{(ia,ib)}$ is the similarity between appliance ia and ib based on the jth feature, M is the total number of features considered, N is the total number of points of feature j, while $y_{k|(ia,j)}$ is a point k of feature j from appliance ia.

We use the air conditioner I as an example to illustrate this concept. Fig. 14 shows the similarity measures based on the CW, PQ, IAW, and STW features, and the corresponding appliance-based accuracy, which is defined in the first part of this two-part paper and used to measure the percentage (probability) of air conditioner I identified as a different appliance herein.

From Fig. 14, it seems that when air conditioner I was operating, the chance of identifying it correctly was 80%, and the chance of recognizing it as other appliances was 20%. With similarity analysis, it can be found that generally the appliances with high similarity with air conditioner I would be misidentified, such as the water boiler (8%) or coffee maker (5%), etc.

VI. Applications

By employing the developed load disaggregation platform, different futuristic applications could be considered. For instance, these may include specific appliance (e.g., air conditioner) tracking, detailed appliance usage recording (appliance operation schedule, energy consumption and CO_2 footprint), and demand side management [8].

Fig. 15(a) shows a typical power profile within 24-hr derived from simulator III. Fig. 15(b) presents the energy consumption for each appliance in the scenario vs the estimates calculated from the results of load signature analysis. Fig. 15(c) shows the estimated on-off status and Fig. 15(d) depicts the CO_2 footprint of several frequently-operated appliances. From the simulation result, it seems that the energy consumption error between the scenario and estimate was small, and the estimated appliance on-off status could match the scenario fairly accurately, especially for those appliances with readily distinguishable features, such as the refrigerator and air conditioners. In essence, such information can be used to help customers in visualizing and identifying ways to conserve or better utilized their appliances and/or dynamic rates if available. For utilities, such knowledge could enhance their load forecasting [9], demand response [10], smart metering [11] and emergency response planning and operations. Moreover, some innovative services, such as equipment health monitoring, may also be provided.

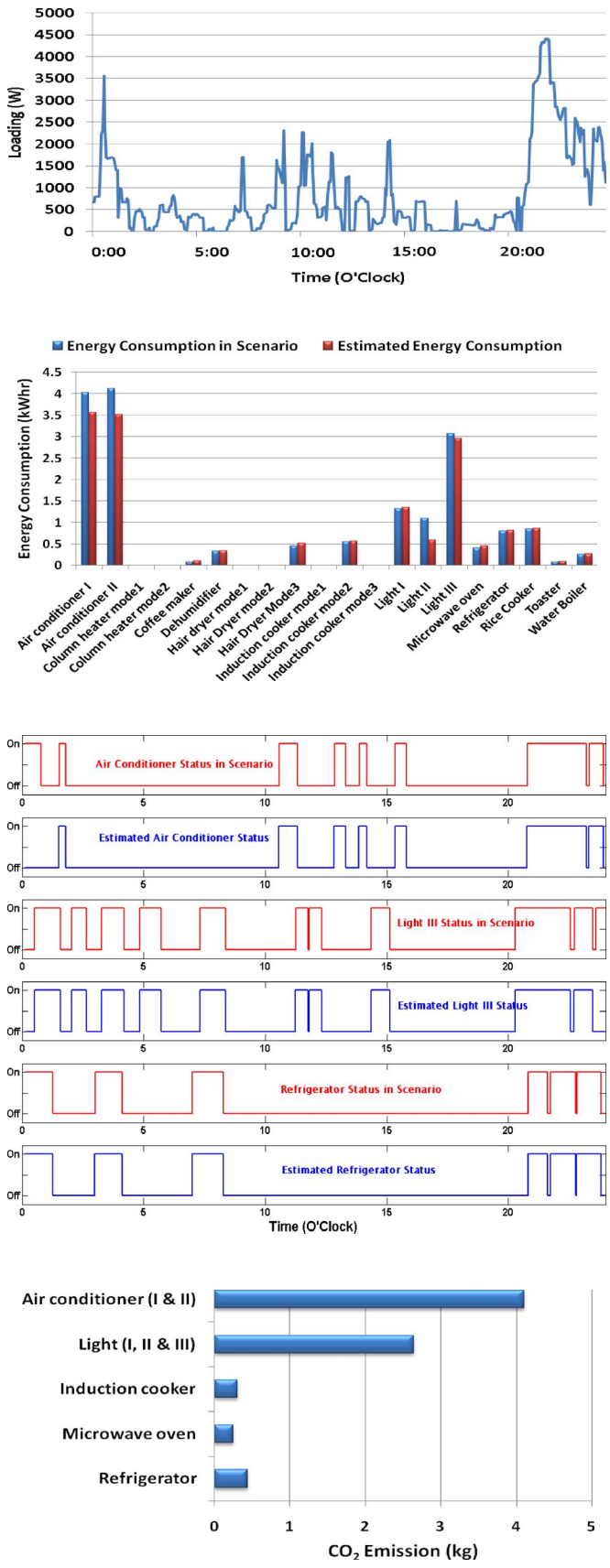

Fig. 15. (a). Power profile within 24-hr. (b). Energy consumption of each appliance in scenario versus estimates. (c). Appliance on-off status in scenario versus estimates. (d). Estimated appliance carbon footprint.

TABLE I
TYPE OF APPLIANCE FOR SIMULATOR III

Type of appliance	Operating duration	Number of occurrence per case	Examples
Type A	Fixed	Fixed	Rice cooker
Type B	Variable	Fixed	Induction cooker and hair dryer
Type C	Fixed	Variable	Toaster and coffee maker
Type D	Variable	Variable	Air conditioner, refrigerator, light and microwave

VII. CONCLUSION

This paper has demonstrated a multi-feature, multi-algorithm disaggregation framework based on load signature analysis and Committee Decision Mechanisms. Using simulations derived from a database composed of common household appliances, all CDMs outperformed other single-feature and single-algorithm disaggregation methods in term of reliability and robustness. Among the different CDMs, Maximum Likelihood Estimation achieved the highest disaggregation accuracy of 92.7% for the given set of appliances and the simulated environment, almost 10% improvement in comparison to the best result from any individual feature-algorithm.

Through the in-depth studies described in the paper, we demonstrate that load signature analysis has the potential to detect the unique consumption pattern of each individual electrical appliance. By applying the load disaggregation techniques, we believe that more intelligent contents could be derived in future, for the purpose of smart metering and/or creating new value for customers and utilities.

APPENDIX

Simulator III:

Classification of Appliances: Four types of appliances with different operating characteristics are defined as Table I:

Procedures:

1) For a predefined case (e.g., 24 h for a daily simulator), 24 h can be divided into different time segments (up to five in this example).
2) For each time segment, we can assign the probability that an appliance is likely to be on (state 1) (e.g., 0.2 for segment 1 (1 P.M. – 3 P.M.)). 0.4 for segment 2 (5 P.M. – 7 P.M.), 0.2 for segment 3 (8 P.M. – 9 P.M.), 0.1 for segment 4 (10 P.M. – 11 P.M.) and 0.1 for segment 5 (1 A.M. – 3 A.M.). It should be noted that the sum of probability for all segments of every appliance should be equal to unity.
3) For the appliance mentioned before, if the random number is drawn to be less than 0.2 in any time in segment 1, it will be on. Otherwise, it will be off and so on for other appliances. The aforementioned process only determines the randomness of an appliance's on time, and the off time is based on the type of appliance as mentioned in the previous subsection.
4) The aforementioned procedures are repeated for other appliances to schedule the on/off sequence accordingly.
5) The other time segment (e.g., segment 2) repeats the aforementioned two steps.

REFERENCES

[1] G. W. Hart, "Nonintrusive appliance load monitoring," *Proc. IEEE*, vol. 80, no. 12, pp. 1870–1891, Dec. 1992.

[2] C. Laughman, K. Lee, R. Cox, S. Shaw, S. Leeb, L. Norford, and P. Armstrong, "Power signature analysis," *IEEE Power Energy Mag.*, vol. 1, no. 2, pp. 56–63, 2003.

[3] K. Suzuki, S. Inagaki, T. Suzuki, H. Nakamura, and K. Ito, "Nonintrusive appliance load monitoring based on integer programming," in *Proc. SICE Annu. Conf.*, Aug. 2008, pp. 2742–2747.

[4] M. Akbar and D. Z. A. Khan, "Modified nonintrusive appliance load monitoring for nonlinear devices," in *Proc. IEEE Int. Multitopic Conf.*, Dec. 2007, pp. 1–5.

[5] S. Drenker and A. Kader, "Nonintrusive monitoring of electric loads," *IEEE Computer Appl. Power*, vol. 12, pp. 47–51, 1999.

[6] R. Billinton and W. Li, *Reliability Assessment of Electric Power Systems Using Monte Carlo Methods*. New York: Plenum, 1994.

[7] Hong Kong Energy End-Use Data 2007 Hong Kong, Elect. Mechan. Services Dept., 2008.

[8] J. W. M. Cheng, G. Kendall, and J. S. K. Leung, "Electric-load intelligence (E-LI): Concept and applications," in *Proc. IEEE Region 10 Conf.*, Hong Kong, China, Nov. 2006, pp. 1–4.

[9] H. Daneshi and A. Daneshi, "Real time load forecast in power system," in *Proc. 3rd Int. Conf. Electric Utility Deregulation Restructuring and Power Technologies*, Apr. 2008, pp. 689–695.

[10] M. H. Albadi and E. F. El-Saadany, "Demand response in electricity markets: An overview," in *Proc. IEEE Power Eng. Soc. General Meeting*, Jun. 2007, pp. 1–5.

[11] C. Bennett and D. Highfill, "Networking AMI smart meters," in *Proc. IEEE Energy 2030 Conf.*, Nov. 2008, pp. 1–8.

Jian Liang received the B.Eng. and M.Eng. degrees in automation from Tsinghua University, Beijing, China, in 2000 and 2003, respectively, and the Ph.D. degree in mechanical and automation engineering from The Chinese University of Hong Kong, Hong Kong, China, in 2006.

His research interests are power and energy technologies. He has applied for one patent, and has been published in many papers. He is a Reviewer for *Energy*, *Energy & Buildings*, *International Journal of . Control & Intelligent Systems*, and others. Currently, he is the Low Carbon Technology Scientist with CLP Research Institute Ltd., Hong Kong.

Simon K. K. Ng (M'06) received the B.Eng. (Hons.) and M.Phil. degrees in electrical engineering from The University of Hong Kong, Hong Kong, China, in 2005 and 2007, respectively, where he is currently pursuing the Ph.D. degree in power systems.

He was a Modeling Specialist with the CLP Research Institute Ltd. from 2008 to 2009. His main research activities include load signature analysis and system health monitoring techniques.

Gail Kendall received the B.Sc. and M.Sc. degrees from the University of California at Berkeley, in 1973 and 1974, respectively, and the Ph.D. degree in mechanical engineering from the Massachusetts Institute of Technology, Cambridge, in 1978.

She is a registered Professional Engineer, a Fellow of HKIE, and an Honorary Fellow with the Energy Institute. Before joining the CLP Research Institute Ltd., she held a number of positions, including Professor of the Practice of Mechanical Engineering at the Massachusetts Institute of Technology and Director of Strategic Science and Technology for the Electric Power Research Institute. She was the Managing Director of the CLP Research Institute Ltd. and was Director of the Group Environmental Affairs with CLP Holdings Ltd. until her retirement in 2008.

John W. M. Cheng (M'98) received the B.Eng. degree in electrical engineering from the University of Saskatchewan, Saskatoon, SK, Canada in 1982, and the M.Eng. and Ph.D. degrees in electrical engineering from McGill University, Montreal, QC, Canada, in 1985 and 2000, respectively.

He is a registered Professional Engineer (P.Eng.) in Ontario and a member of CIGRE and HKIE. His current research interests include load signature analysis, smart meters, energy technologies in buildings, and simulation techniques. Currently, he is the Manager of Low Carbon Tech–R&D in the Carbon Ventures Group of CLP Holdings, Hong Kong.